Progress in Organic Coatings 123 (2018) 185–189

Contents lists available at ScienceDirect

Progress in Organic Coatings

journal homepage: www.elsevier.com/locate/porgcoat

Zinc-reduced graphene oxide for enhanced corrosion protection of zinc-rich epoxy coatings

Shuai Teng[a,1], Yang Gao[b,c,1], Fengli Cao[a], Debin Kong[b], Xiaoyu Zheng[d], Xiaomei Ma[a,*], Linjie Zhi[b,*]

[a] School of Chemistry and Chemical Engineering, Qingdao University, Qingdao, 266071, China
[b] Key Laboratory of Nanosystem and Hierarchical Fabrication, National Center for Nanoscience and Technology, Beijing, 100190, China
[c] School of Chemical Engineering and Technology, Tianjin University, Tianjin, 300072, China
[d] Institute of Forensic Science, Ministry of Public Security, Beijing, 100038, China

ARTICLE INFO

Keywords:
Zinc-rich coating
Reduced graphene oxide
Corrosion protection
Electrochemical impedance spectroscopy

ABSTRACT

Zinc-reduced graphene oxide (Zn/rGO) is introduced into zinc-rich coatings (ZRCs) to enhance the anticorrosion performance. The interaction between zinc powder and graphene oxide (GO) nanosheets can simultaneously realize the reduction of GO and the dispersion of rGO nanosheets. Scanning electron microscopy, potentiodynamic polarization, electrochemical impedance spectroscopy (EIS) and salt spray test are used to characterize the corrosion protection performance of coatings. The results of coating morphology, electrochemical measurements and salt spray test demonstrate that the well-dispersed rGO nanosheets decrease the coating porosity and provide effective protectiveness for zinc particles, thus Zn-rGO/ZRC generating improved barrier property against aggressive species and long-term cathodic protection ability as compared to other coatings.

1. Introduction

Zinc-rich coatings (ZRCs), as an effective organic anticorrosion coating, have been utilized in many industrial environments to protect the metals away from aggressive species, even mechanical damage occurring [1,2]. The value of pigment volume concentration (PVC) for ZRCs has been reported to markedly affect the mechanism of corrosion protection for ZRCs [3,4]. The barrier property rather than cathodic protection dominates the protection mechanism of ZRCs with a PVC lower than the critical pigment volume concentration (CPVC). While a sufficient amount of zinc particles is added to the resin matrix to reach a higher PVC value than 60 or the CPVC, the cathodic protection determines the protection mechanism of ZRCs in consequence of the continuous electrical contact between zinc particles and steel substrate [5–7]. However, a high quantity of zinc particles can deteriorate coating flexibility, adhesion force to the steel substrate and tortuosity of diffusion pathways [8]. In this respect, there are some methods to enhance electrical conductivity of coatings with a lower amount of zinc particles, a common one of which is using carbon-based conductive fillers, such as carbon black [9], carbon nanotubes [10,11], graphene oxide [6], and graphene [8]. Nevertheless, the dispersion of conductive fillers and the contact between conductive fillers and zinc particles are still not enough to get the optimal result.

As an emerging two dimensional (2D) materials, graphene has gained plenty of attention derived from its unique properties such as large mechanical strength, high thermal and electrical conductivity, large surface area, super hydrophobic property and good flexibility [12,13]. There have been several investigations focusing on the effect of graphene on the anticorrosion performance of organic coatings [14,15]. The individual 2D nanolayer structure of graphene endows coatings with good inhibitive ability and excellent impermeability to aggressive species. Additionally, the existence of graphene nanosheets in ZRCs can effectually provide continuous electrical contact between zinc particles and steel substrate and thus improve the electrical percolation of the coatings even with a lower amount of zinc particles. However, graphene nanosheets are prone to aggregating together attributed to their strong van der Waals forces and large surface areas, which degrades corrosion protection capability of ZRCs and hinders homogeneous dispersion of graphene in resin matrix [16]. Attempts to improve dispersion of graphene in composite coatings always involve chemical modification of graphene [17]. Another alternative to reach good dispersion of graphene is using GO followed by reduction. Taking into account the ability that zinc powder can effectively reduce GO at room temperature [18,19], it is reasonable to use zinc powder as the reductant of GO, thus

* Corresponding authors.
E-mail addresses: mxm@qdu.edu.cn (X. Ma), zhilj@nanoctr.cn (L. Zhi).
[1] These authors have contributed equally to this work.

https://doi.org/10.1016/j.porgcoat.2018.07.012
Received 16 May 2018; Received in revised form 29 June 2018; Accepted 7 July 2018

simultaneously achieving the dispersion of rGO nanosheets and the preparation of composite pigment, Zn/rGO. However, there is few report on using Zn/rGO in the corrosion protection ability of ZRCs.

In this work, zinc powder was employed to perform the reduction of GO, assisted by ultrasonication, to prepare Zn/rGO composite pigment with good dispersion of rGO nanosheets. When Zn/rGO was introduced to epoxy resin ZRCs, the obtained Zn-rGO/ZRC revealed excellent corrosion protection performance with a lower amount of zinc particles, only about 40 wt%. The introduction of Zn/rGO is able to promote the anticorrosive performance of ZRCs, which is derived from (1) good dispersion of rGO nanosheets, (2) effective protectiveness for zinc particles from rGO nanoflakes, which imparts ZRCs to long-term galvanic protection ability, and (3) high barrier properties of rGO nanosheets.

2. Experimental

2.1. Materials

Q-215 steel sheets (from Guangzhou Biuged Instruments, China) with the nominal chemical composition (wt%) of C 0.15, Mn 1.20, Si 0.35, P 0.045, S 0.045 and Fe balance were employed to appraise the anticorrosion performance of ZRCs. GO was obtained through a modified Hummer's method. A commercial zinc-rich epoxy primer composed of epoxy resin and curing agent was purchased from The Forbidden City Paint Industry, China. The zinc-rich epoxy primer contains 40 wt% zinc particles. Graphene was purchased from 2D Carbon (Changzhou) Tech. Inc. Ltd, China. N,*N*-dimethylformamide (DMF) and polyvinyl pyrrolidone (PVP) (from Sigma-Aldrich) were used to prepare the dispersion of graphene. Zn powder and hydrochloric acid (36%–38%) were purchased from Sinopharm Chemical Reagent Co. Ltd, China.

2.2. Preparation of coating samples

The required amount of obtained GO aqueous solution with a solid content of 17.7 wt% was added to zinc-rich epoxy primer to prepare GO/ZRC coating with 1 wt% GO content.

For the preparation graphene/ZRC, the purchased graphene nanosheets was dispersed in PVP-DMF solution under ultrasonic condition. Then, the required amount of graphene solution was added to zinc-rich epoxy primer to prepare graphene/ZRC coating with 1 wt% graphene content.

To prepare the sample of Zn-rGO/ZRC, the reduction of GO was performed firstly. With a mass ratio of GO to Zn of 1/4, 0.6 g of Zn powder was added to 0.85 g of GO solution. After 30 min of ultrasonication, Zn/rGO was obtained and then the required amount of Zn/rGO was added to zinc-rich epoxy primer to prepare Zn-rGO/ZRC coating with 1 wt% rGO content.

2.3. Characterization

The morphology was characterized by scanning electron microscopy (SEM, Hitachi S4800). X-ray diffraction (XRD) and Raman spectra were collected by Rigaku D/max-2500B2 + /PCX system and Renishaw inVia Raman microscope, respectively.

The electrochemical measurements of various ZRCs were tested by a standard three-electrode system, adapting KCl saturated Ag/AgCl electrode and graphite electrode as reference electrode and counter electrode, respectively. The exposed area was around 35 cm^2. All measurements were carried out in 3.5 wt% NaCl solution employing a Bio-logic VMP potentiostat workstation. EIS measurement was conducted at open circuit potential (OCP) in the frequency range of 100 kHz to 10 mHz with a signal amplitude of 10 mV. Before EIS measurement, an OCP measurement was performed to reach a stable OCP. Zview software (Version3.1) was used to analyze EIS results.

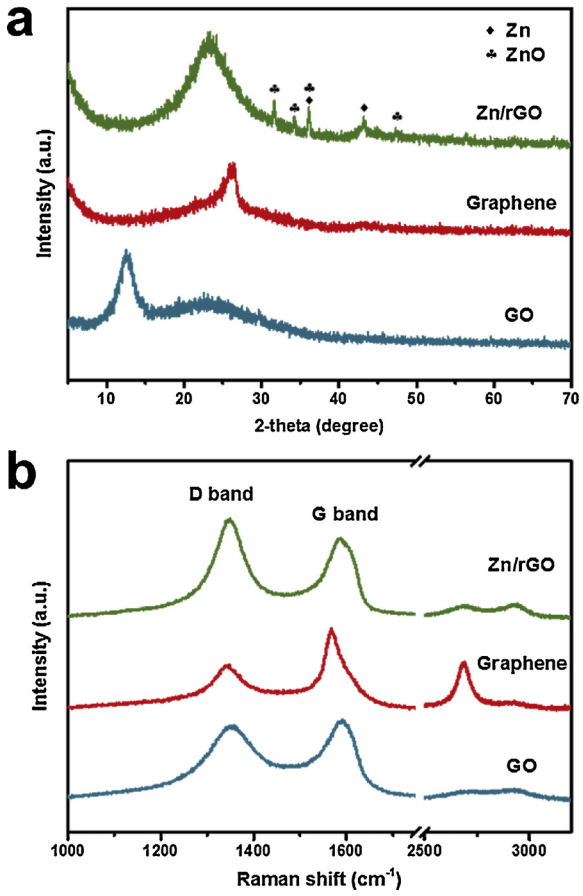

Fig. 1. (a) XRD patterns and (b) Raman spectra of GO, graphene and Zn/rGO.

Polarization curves were performed with 1 mV/s sweeping rate and scanned from −0.15 V below OCP to 0.15 V above OCP.

Salt spray test was conducted in a salt spray chamber (Dongguan Zhongzhi Testing Instruments Co. Ltd, China) according to the Chinese standard GB/T 1771-1991. A 3.5 wt% NaCl solution was used for salt spray test with a constant chamber temperature of 35 °C. The surface morphology and the scratch line width of the coatings were tested by video measuring instrument (Guiyang Xintian OETEOH. Ltd, China).

3. Results and discussion

3.1. Zn/rGO characterization

XRD patterns of GO, graphene and Zn/rGO are shown in Fig. 1a. Due to the presence of abundant oxygen-containing functionalities and intercalated water molecules between GO nanosheets, the diffraction peak of GO was located at 12.6° assigned to the basal spacing of 7.02 Å. After the treatment of zinc powder under ultrasonication, Zn/rGO displays a broad diffraction peak at 23.3° close to that of purchased graphene, indicating the partial recovery of the graphite crystal structure. Additionally, the peaks of Zn (zinc, JCPDS 04-0831) and ZnO (zincite, JCPDS 36–1451) can also be observed in Zn/rGO, which is derived from the partial oxidation of zinc interacted with GO. As given in Fig. 1b, Raman spectra exhibits two main bands, of which D and G bands are associated with breathing mode of A_{1g} symmetry and E_{2g} symmetry of sp^2 carbon atoms, respectively [20]. After the chemical reduction of zinc, the characteristic D band (1353 cm^{-1}) and G band (1592 cm^{-1}) of GO are shifted to 1348 cm^{-1} and 1586 cm^{-1}, respectively. The D band of rGO increases prominently due to the increase in the amount of isolated sp^2 domains [21,22], resulting in that the intensity ratio of the D and G bands, I_D/I_G, increases from 0.92 to 1.23. Besides, the Raman